# Applicability of Total Horizontal Potential-Difference Magnitude to 2D Inversion for Dipole-Dipole Array Data in Complex 3D Structures with Strong Resistivity Contrasts

Churl Hyun Jo*

*Director of Research Division, Subsurface Information Technologies, Inc., D 609, 40 Imee-ro, Uiwang-si, Gyeonggi-do, Republic of Korea. Email: chjo@geeha.co.kr

**ABSTRACT**

Complex 3D subsurface structures with strong resistivity contrasts can cause the horizontal electric field to deviate substantially from the survey-line direction. Under such conditions, conventional 2D electrical resistivity tomography (ERT), which relies only on the inline potential-difference component, may yield incomplete inversion results. Although full 3D interpretation using the horizontal electric-field vector is in principle more appropriate, practical limitations remain in field acquisition and inversion capability. This study therefore examines an intermediate approach in which the total horizontal potential-difference magnitude (Vt), obtained from two-component ERT measurements, is applied to conventional 2D inversion software. Numerical experiments were conducted using dipole–dipole array data generated for a complex 3D conductive anomaly model with strong resistivity contrast, and Vt-based 2D inversion results were compared with conventional results based on the inline component (Vx). The results show that, where localized 3D distortion of the horizontal electric field is significant, Vt inversion provides clearer separation of adjacent conductive anomalies than Vx inversion. This difference becomes more pronounced as the resistivity contrast increases. In contrast, no pronounced difference is observed between the two inversion results for structures exhibiting quasi-2D behavior. However, some Vt inversion sections show more pronounced edge-related artifacts. Thus, under the dipole–dipole array conditions examined in this study, Vt-based 2D inversion should not be regarded as universally superior, but may provide complementary information to conventional Vx-based interpretation where strong resistivity contrasts and localized 3D structural changes cause large deviations in horizontal electric-field direction.

**KEY WORDS:** Electrical resistivity tomography (ERT), 3D structures, two-component measurement, total horizontal potential difference, dipole-dipole array, 2D inversion

## INTRODUCTION

Electric fields generated by subsurface anomalies with complex 3D geometries and strong resistivity contrasts relative to the background medium naturally exhibit complex spatial distributions. In particular, the horizontal electric field at the ground surface does not always coincide with the survey-line direction, and near anomaly terminations or locations where geometry changes abruptly, its direction may deviate substantially from the survey line. Under such conditions, it is reasonable to question how adequately subsurface structure can be evaluated using only the inline potential-difference component measured along a straight survey line, as is common in conventional ERT surveys.

This question does not imply that conventional ERT interpretation lacks practical value. In field applications, ERT is often conducted not to reconstruct complex targets in detail, but to determine their presence or to obtain an approximate picture of geological conditions. From this perspective, conventional 2D ERT interpretation based only on the inline component has provided sufficiently useful information in many cases. Even when the electric field deviates to some degree from the survey-line direction, the presence of a conductive anomaly may still be reflected in the observations, and interpretation results adequate for practical purposes can often be obtained.

However, the fact that conventional methods have been practically successful does not mean that information contained in the unmeasured horizontal component is unimportant. When complex 3D structure is combined with strong resistivity contrast, changes in electric-field direction can become large, and the inline component alone may fail to represent adequately the location, continuity, or separation of adjacent anomalies. It is therefore worthwhile to examine the extent to which considering the previously neglected horizontal component can provide additional and useful information to complement conventional ERT interpretation.

The potential improvement of 3D ERT through horizontal electric-field vector measurements was proposed by Jo and Cho (2025). That study presented the conceptual possibility of measuring both the magnitude and direction of the horizontal electric field and using them in 3D interpretation. However, the work remained largely theoretical and was not validated with field examples or full 3D inversion. Moreover, fully utilizing horizontal electric-field vector data fundamentally requires horizontal electric-field measurements, 3D survey layouts, and 3D inversion. In practice, field implementation of 3D ERT based on horizontal electric-field vector measurements involves substantial difficulties. Even conventional 3D ERT using only inline components is demanding in terms of field operations and data processing; adding horizontal vector measurements would further increase the complexity of electrode layouts, cable configurations, measurement channels, and field support. In addition, inversion algorithms and interpretation software capable of directly processing such data have not yet been reported to be generally available. Therefore, widespread application of full 3D ERT based on horizontal electric-field vector measurements is likely to require considerable time.

Nevertheless, until full 3D vector ERT surveys and interpretation become feasible, it is worthwhile to consider intermediate ways of utilizing horizontal electric-field vector data. In this study, we examine the use of the total horizontal potential-difference magnitude (Vt), obtainable from two-component ERT measurements, as input to conventional 2D inversion software. Here, Vt denotes the total horizontal potential-difference magnitude calculated by combining the inline potential-difference component (Vx) with the orthogonal horizontal component. Conventional 2D ERT interpretation is itself essentially an approximate approach that selects and interprets only the inline component from the electric-field response generated by a 3D subsurface structure. From this perspective, even without using directional information from the horizontal electric-field vector, applying only its magnitude information to an existing 2D inversion framework may be a viable approach.

The purpose of this study is to examine how Vt-based 2D inversion differs from conventional Vx-based 2D inversion and whether such differences can provide meaningful interpretational information. To this end, conductive anomaly models with strong resistivity contrasts and complex 3D geometries were constructed, and Vx and Vt data were generated by 3D numerical modeling under dipole-dipole array conditions. The two datasets were then inverted using the same 2D inversion software so that the applicability and limitations of Vt-based 2D inversion could be evaluated.

## APPLICATION OF TWO-COMPONENT SINGLE-LINE DATA TO 2D INVERSION

### 3D Anomaly Model

To examine the intermediate approach described above, a conductive anomaly model with complex 3D geometry was constructed (Fig. 1). The background was assumed to be homogeneous, and a conductive anomaly with much lower resistivity than the background medium was embedded within it. A horizontal overburden layer was added at the top to provide a modest degree of realism.

The conductive anomaly has an arrow-shaped plan-view geometry and is not intended to reproduce a specific geological structure. Rather, it is a hypothetical model designed to examine how strong resistivity contrast and localized 3D geometric changes can affect the horizontal electric field in zones where the geometry changes abruptly, such as near the tip of an arrow-shaped body. The model geometry and major numerical-modeling parameters are summarized in Table 1.

Particular attention was given to anomaly terminations and other zones of abrupt geometric change. At such locations, the influence of the conductive anomaly can cause large changes in horizontal electric-field direction. Accordingly, substantial differences may arise between conventional Vx measurements and measurements of the total horizontal potential-difference magnitude Vt.

**Table 1. Numerical modeling parameters used in the synthetic example.**

| Parameter | Value / Description |
|---|---|
| Numerical method | 3D finite-element method (FEM) |
| Solver | PARDISO direct sparse solver |
| Core grid size | Nx=121, Ny=49, Nz=41 |
| Grid spacing | 2.5 m uniform spacing in the core model; padding spacing increases outward by factors of 2, 4, 8, and 16, with a maximum spacing of 40 m |
| Host medium resistivity | 1 kΩ·m (base case); 100 Ω·m and 10 kΩ·m for contrast tests |
| Overburden | 100 Ω·m, 10 m thick, flat layer |
| Conductive anomaly | Arrow-shaped body, 1 Ω·m, extending from 10 to 80 m depth; horizontal width = 10 m |

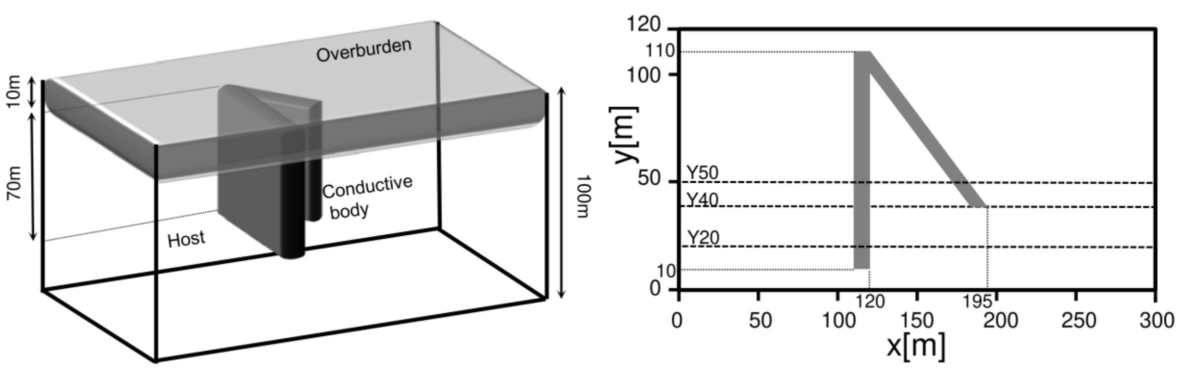


Fig. 1. Synthetic 3D conductive anomaly model used in this study. (a) Three-dimensional view of the arrow-shaped conductive body beneath a 10 m thick horizontal overburden layer. The conductive body extends from 10 to 80 m depth within a homogeneous host medium. (b) Plan view of the model showing the arrow-shaped anomaly and representative survey lines used for 2D inversion comparison.

### Survey Configuration and Inversion Procedure

Synthetic survey data were generated by 3D numerical modeling of the conductive anomaly model described above. A dipole-dipole array was adopted. This array was selected because it was considered an array condition in which differences between Vx and Vt data could appear relatively clearly. By contrast, in arrays where the potential-electrode pair is located between the current electrodes, such as the gradient array, the dominant electric field may be oriented largely along the current-electrode axis, reducing the contribution of the transverse component. Consequently, the difference between Vx and Vt data may be relatively limited in such array geometries.

Figure 2 schematically illustrates the inline and transverse potential-difference measurements. The conventional inline potential-difference component is defined as the potential difference measured by the inline electrode pair Mx-Nx, whereas the transverse potential-difference component is defined as the potential difference measured by the transverse electrode pair My-Ny. The total horizontal potential-difference magnitude is then calculated by combining the inline potential-difference component with the orthogonal transverse component.

$$\Delta V_x = V_{Mx} - V_{Nx}, \quad \Delta V_y = V_{My} - V_{Ny} \tag{1}$$

$$\Delta V_t = \sqrt{(\Delta V_x^2 + \Delta V_y^2)} \tag{2}$$

For convenience, $\Delta V_x$ and $\Delta V_t$ are hereafter denoted by Vx and Vt, respectively. In Vx-based 2D inversion, ΔVx in Eq. (1) is used as the input data. In Vt-based 2D inversion, ΔVt is calculated from ΔVx and ΔVy using Eq. (2) and is then used as the input data.

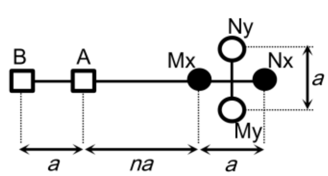


Fig. 2. Schematic illustration of the inline and transverse potential-difference measurements for a dipole-dipole array.

Survey lines were oriented along the x axis, and the number in each line name denotes its y coordinate. All lines extended from x = 0 m to x = 300 m. Survey lines were placed at 10 m intervals from Y10 to Y110, and both Vx and Vt datasets were generated for each line. Figure 1(b) shows the model in plan view together with representative survey lines.

The Y10 to Y30 lines mainly intersect one conductive anomaly, whereas the Y40 to Y110 lines intersect two conductive anomalies. Among these, the Y40 line passes through a location corresponding to the termination of one of the two anomalies and therefore crosses a zone of particularly pronounced spatial change. In contrast, the Y110 line passes through the zone where the two anomalies merge into a single continuous structure.

The generated Vx and Vt datasets were separately input to the same 2D inversion software. The commercial 2D inversion program DIPRO, based on the algorithm of Yi et al. (2003), was used. To isolate differences caused only by the input data type, identical inversion parameters and imaging conditions were applied to both inversions. The discussion focuses mainly on the Y20, Y40, and Y50 survey lines, for which relatively clear differences between Vx and Vt results were observed. Arrows shown on the inversion sections indicate the locations where the survey line intersects the conductive anomalies.

**Comparison of Vt and Vx Inversion Results**

Figure 3 compares representative 2D inversion results obtained from Vt and Vx data. Because identical inversion and display conditions were applied to the two datasets, differences between the inversion sections can be attributed to whether Vt or Vx was used as input. A general feature of the inversion results is that, where a survey line crosses both the shaft and the head of the arrow-shaped anomaly, low-resistivity zones tend to form a connection between the two anomalies. This can be understood as the combined influence of the two conductive bodies being represented as a single low-resistivity response during 2D inversion.

The Y50 inversion results are shown in Figs. 3(a) and 3(b). In the Vt inversion section, the low-resistivity anomaly tends to divide into two zones near the locations where the survey line crosses the two conductive bodies. Although the positions of the low-resistivity minima do not exactly coincide with the true anomaly locations, the indication that two separate bodies may be present is relatively clear. In contrast, the Vx inversion section shows a single broad connected low-resistivity zone, and separation of the two conductive bodies is not clearly expressed. Although some potential for separation can be inferred from near-surface contour patterns, the distinction is much weaker than in the Vt inversion.

The Y40 inversion results are shown in Figs. 3(c) and 3(d). This line passes through the termination zone of a conductive body and therefore crosses a location of strong spatial variation. In the Vt inversion result, low-resistivity zones corresponding to the two conductive bodies are

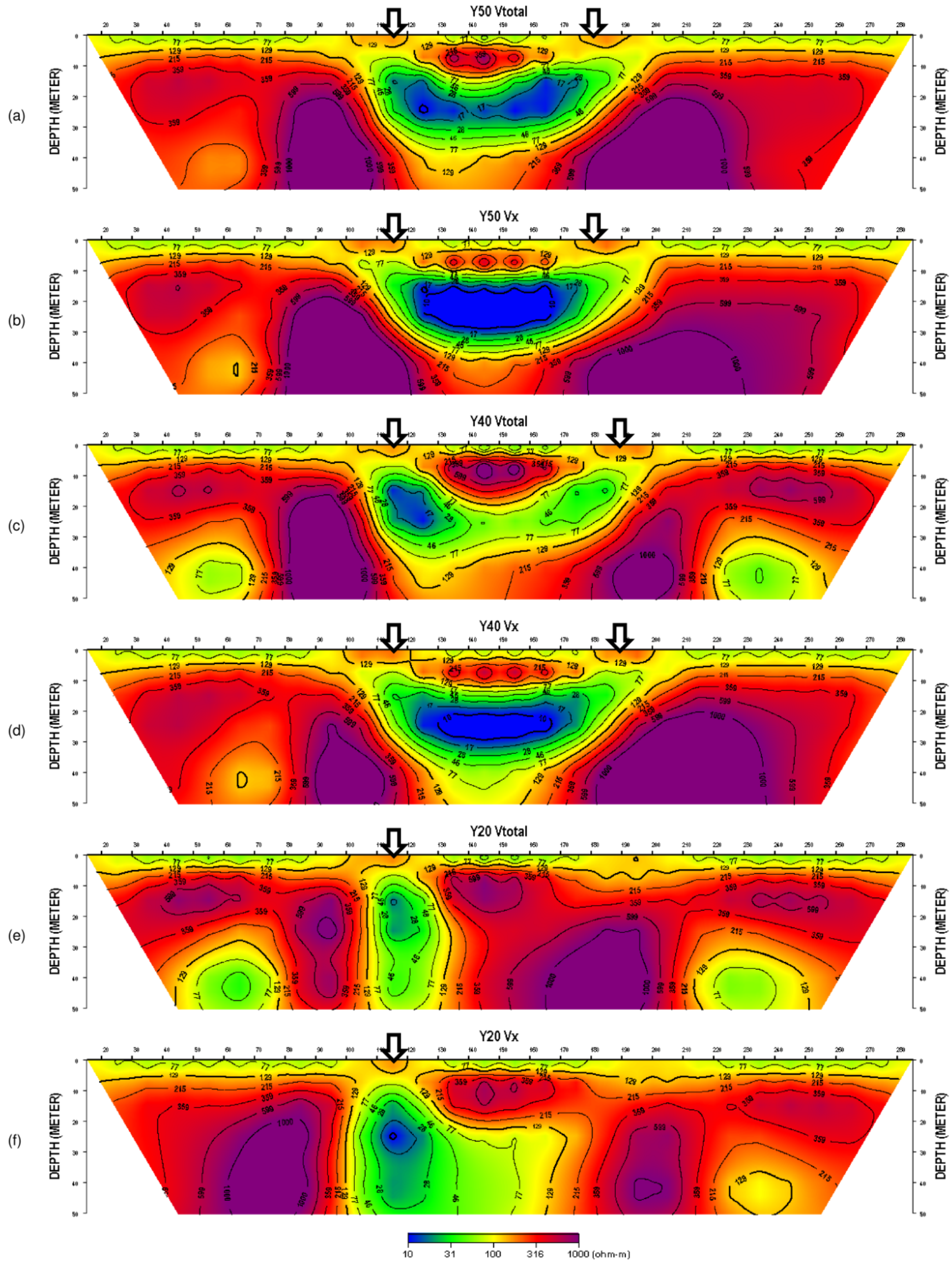


Fig. 3. Comparison of 2D inversion results obtained from Vt and Vx data along representative survey lines: (a) and (b) Y50, (c) and (d) Y40, and (e) and (f) Y20. Panels (a), (c), and (e) show Vt-based inversion results, whereas panels (b), (d), and (f) show Vx-based results. Arrows indicate the intersections of the survey lines with the conductive anomalies.

relatively clearly separated. In contrast, as in the Y50 result, the Vx inversion shows a low-resistivity zone spread broadly along the survey-line direction, and separation of the two conductive bodies is not clearly represented.

The Y20 line intersects only one conductive body, and the inversion results are shown in Figs. 3(e) and 3(f). In the Vt inversion section, the low-resistivity anomaly is concentrated near the true anomaly location. In the Vx inversion section, a low-resistivity minimum occurs at the anomaly location, but the low-resistivity zone also extends a considerable distance along the survey line, potentially giving the impression that the actual anomaly is more laterally continuous than it is. In this sense, the Vx inversion section appears to reflect more strongly the influence of the anomaly located above the section. A similar difference was observed along the Y30 survey line.

For the remaining lines, namely Y10 and Y60-Y110, no pronounced difference was observed between Vt and Vx inversion results. Along Y10 and Y110, both methods produced low-resistivity anomalies concentrated near the anomaly locations. Along Y60-Y100, neither method could separate the two anomalies; as in the Y40 and Y50 Vx inversion results, the low-resistivity minimum occurred between the two anomalies and the low-resistivity zone spread into the surrounding region.

These results indicate that, in zones where complex 3D geometry combined with strong resistivity contrast produces large changes in horizontal electric-field direction, inversion based only on the inline component may fail to represent adequately the separation of anomalies. By contrast, even when conventional 2D inversion software is used, inversion of total horizontal potential-difference magnitude data can, in some zones, show the separation of adjacent conductive anomalies more clearly. In other words, in zones of large electric-field directional change, Vt inversion tends to represent conductive anomalies more compactly than Vx inversion and to show clearer separation of adjacent conductive structures.

However, Vt inversion cannot be regarded as more stable in all respects. In some Vt inversion sections, numerical low-resistivity artifacts unrelated to the actual subsurface structure were more pronounced than in the corresponding Vx inversions. These artifacts appear particularly near section edges, where data coverage is relatively sparse and boundary effects become more significant. This weakness may be mitigated to some extent by jointly comparing and interpreting Vx and Vt inversion results.

**Comparison of Inversion Results for Different Resistivity Contrasts**

The preceding results show that clear differences can arise between Vt and Vx inversions for the base model. However, it is also necessary to examine separately how these differences vary with resistivity contrast between the anomaly and the background medium. Additional numerical-modeling experiments were therefore conducted along the Y40 survey line using different resistivity contrasts. The Y40 line crosses an anomaly termination and showed the clearest difference between Vt and Vx inversions in the base model. The resistivity contrast of the base model is 1000:1. For comparison, a lower-contrast case of 100:1 and a higher-contrast case of 10000:1 were also examined. For the 100:1 case (1 Ω·m conductor and 100 Ω·m background), the overburden and background would otherwise have the same resistivity. To distinguish them, only in this case was the overburden resistivity set to 10 Ω·m; in the other cases it remained 100 Ω·m. The modeling results are shown in Fig. 4.

The inversion results for the relatively low resistivity contrast of 100:1 are shown in Figs. 4(a) and 4(b). Both Vt and Vx inversions distinguish the locations of the two conductive anomalies. In this case, the directional change of the horizontal electric field is relatively small, and Vx data alone appear to provide an adequate level of interpretation.

For the resistivity contrast of 1000:1, a clear difference between the two inversion results was already demonstrated in Figs. 3(c) and 3(d). The inversion results for the larger contrast of 10000:1 are shown in Figs. 4(c) and 4(d). At this larger contrast, the difference between Vt and Vx inversion results becomes more pronounced. In the Vt inversion, the two conductive anomalies appear as relatively independent low-resistivity zones, whereas in the Vx inversion the low-resistivity zone extends more broadly and the two anomalies are not clearly separated. Thus, in the Vx inversion, the influence of the conductive anomalies tends to spread toward the central region between them, whereas in the Vt inversion the response is relatively concentrated around the respective anomaly locations. Low-resistivity anomalies unrelated directly to the actual subsurface structure also appear near both lower ends of the two inversion sections. These numerical inversion artifacts are more pronounced in the Vt section.

These results suggest that the effectiveness of Vt-based 2D inversion is not determined simply by 3D geometry itself, but is related to the extent to which that geometry, when combined with strong resistivity contrast, changes the direction of the horizontal electric field. When resistivity contrast is low or electric-field directional changes are small, Vt and Vx inversion results may not differ greatly. In contrast, when strong resistivity contrast and localized 3D geometric variation occur together, Vt-data inversion can provide more favorable results for distinguishing anomalies that are difficult to separate in conventional Vx-data inversion.

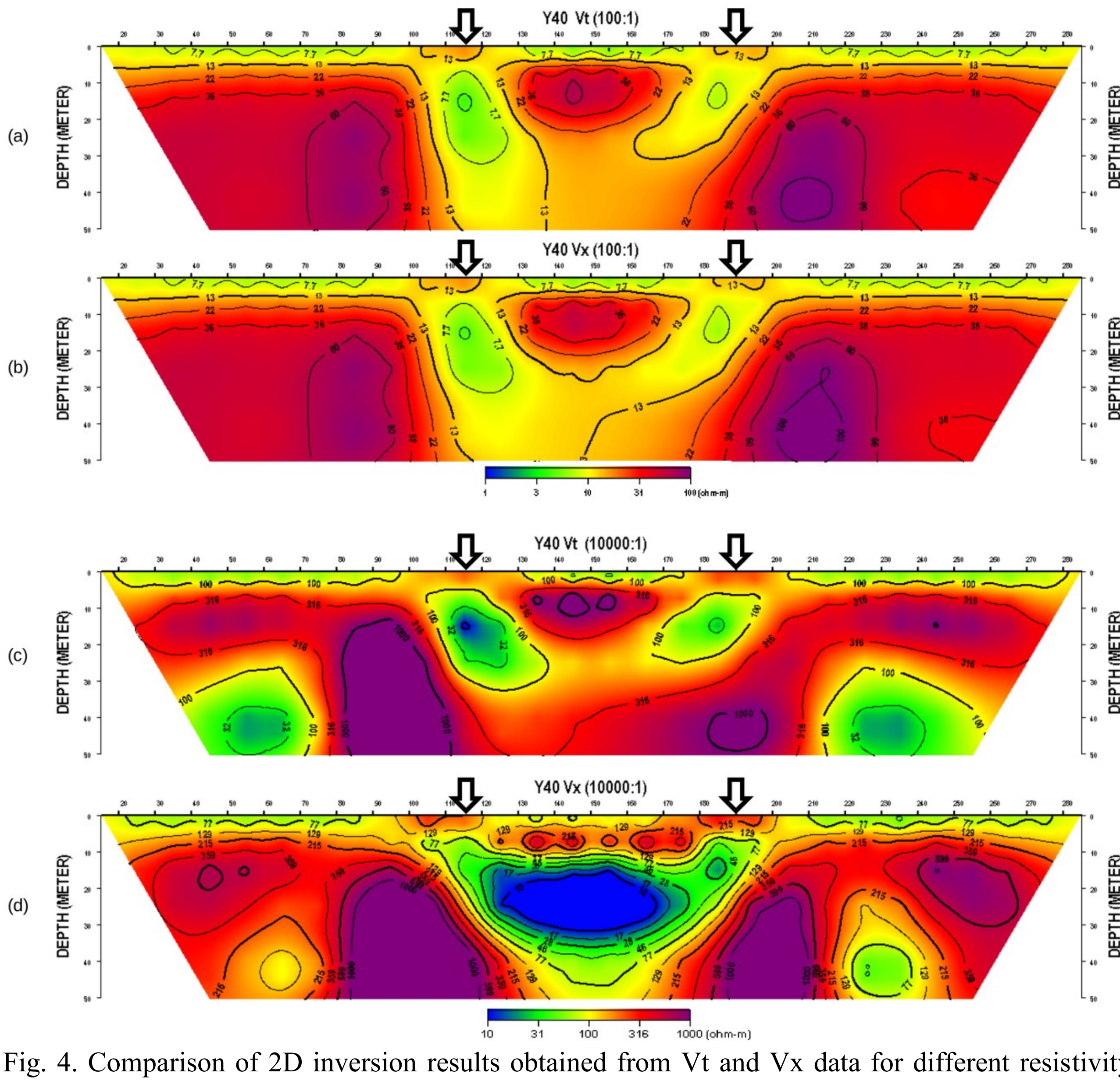


Fig. 4. Comparison of 2D inversion results obtained from Vt and Vx data for different resistivity contrasts along the Y40 survey line: (a) and (b) resistivity contrast of 100:1, and (c) and (d) resistivity contrast of 10000:1. Panels (a) and (c) show Vt-based inversion results, whereas panels (b) and (d) show Vx-based results. A logarithmic resistivity color scale of 1-100 Ω·m is used for panels (a) and (b), whereas a scale of 10-1000 Ω·m is used for panels (c) and (d).

**Comparison of Inversion Results for Quasi-2D Structures**

The arrow-shaped model considered above represents a case with pronounced localized 3D geometric changes, such as the termination of a conductive body. To examine the difference between Vt and Vx inversion results when anomalies develop relatively continuously along or around the survey line and the electric-field response is expected to be closer to that of a 2D structure, two additional quasi-2D models were considered. Here, the term quasi-2D behavior is not intended as a rigorous classification based on a separate dimensionality analysis of the electric field, but rather denotes cases in which the anomaly geometry and continuity suggest a response close to that expected from a 2D structure. The two quasi-2D models are shown in Fig. 5. Both models have a resistivity contrast of 1000:1. Because the inversion results were generally similar, only representative results are shown in Fig. 6.

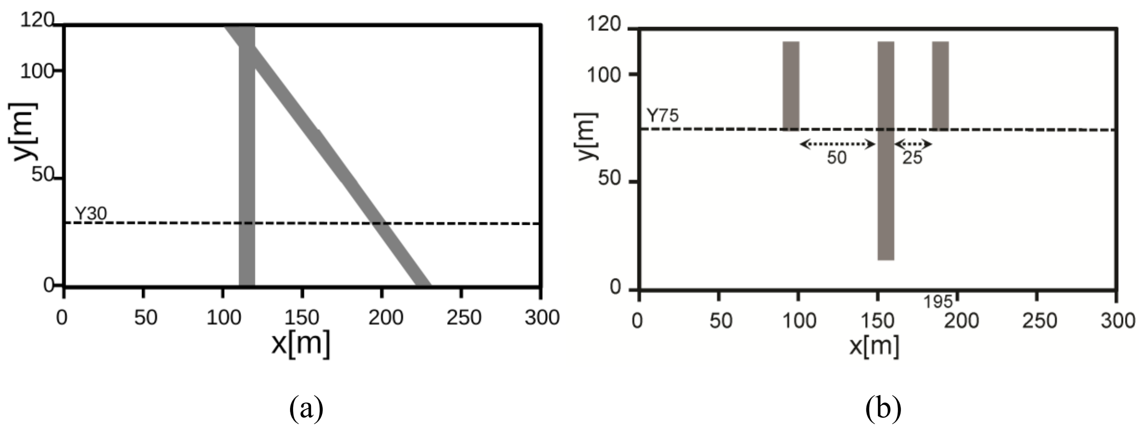


Fig. 5. Quasi-2D conductive anomaly models shown in plan view for comparison of Vt- and Vx-based inversion results: (a) extended arrow-shaped model with sufficiently long anomaly extensions to reduce end effects and (b) parallel conductive anomaly model composed of three bodies elongated in the y direction.

The first model resembles the conductive anomaly model in Fig. 1, but all anomaly segments were given sufficiently long extensions to reduce abrupt termination effects (Fig. 5(a)). Although this model is not a perfectly 2D structure in the strict sense, its anomaly continuity is greater than that of the original arrow-shaped model, so its electric-field response can be regarded as closer to quasi-2D behavior.

Vt and Vx inversions were performed along representative survey lines for this model, and no pronounced difference was observed between the two inversion results. Along Y10 and Y20, where the intersection points between the survey line and the anomalies are sufficiently far apart, both Vt and Vx sections distinguish the anomalies. Along Y30, separation begins to appear in both sections, although the tendency is somewhat clearer in the Vt section (Figs. 6(a) and 6(b)). The right-hand low-resistivity minimum occurs at an x coordinate slightly larger than the actual survey-line intersection. This is interpreted as reflecting the influence of the 3D geometry, in which the anomaly extends in the positive x direction around the survey line. In contrast, along Y40-Y110, where the intersection points are not sufficiently separated, the anomaly zones merge into a single response in both Vt and Vx sections and cannot be distinguished.

The second model consists of parallel conductive anomalies elongated in the y direction (Fig. 5(b)). The overall model dimensions were kept the same as those of the preceding models. The anomalies were oriented perpendicular to the x direction and extended along y. The model comprises three conductive bodies: the two outer bodies have the same limited extent, whereas the central body has a somewhat greater extent. The spacing between anomalies was also varied asymmetrically with respect to the central body. Instead of the Y70 line, Y75 was selected so that the survey line passes through the termination positions of the two outer anomalies.

For the parallel model, responses of the anomalies were observed and distinguished in both Vx and Vt sections for all survey lines examined. Along Y10-Y60, where the survey line intersects only the long central anomaly, the response of that anomaly is dominant. Along Y75-Y110, where the survey line intersects all three anomalies, the three responses are separately expressed. In particular, even along Y75, which passes through the terminations of the two outer anomalies, the locations of the individual anomalies are clearly distinguished in both Vx and Vt sections (Figs. 6(c) and 6(d)). These comparisons indicate that when anomalies have relatively simple 2D continuity with respect to the survey line, conditions approach those assumed by conventional 2D inversion, and structural separation can be achieved satisfactorily using Vx inversion alone.

**Synthesis of Results**

The results of the preceding analyses show that the effectiveness of Vt-based 2D inversion is not determined simply by the geometric complexity of an anomaly. The key factor is the extent to which the 3D geometry of the anomaly changes the direction of the horizontal electric field. When the electric-field response is close to quasi-2D behavior, differences between Vt and Vx inversion results are small, and the structure can be resolved relatively well by conventional 2D inversion alone. In contrast, when strong resistivity contrast occurs together with localized 3D geometric changes, Vt inversion can represent more clearly anomaly separation that remains ambiguous in conventional Vx inversion.

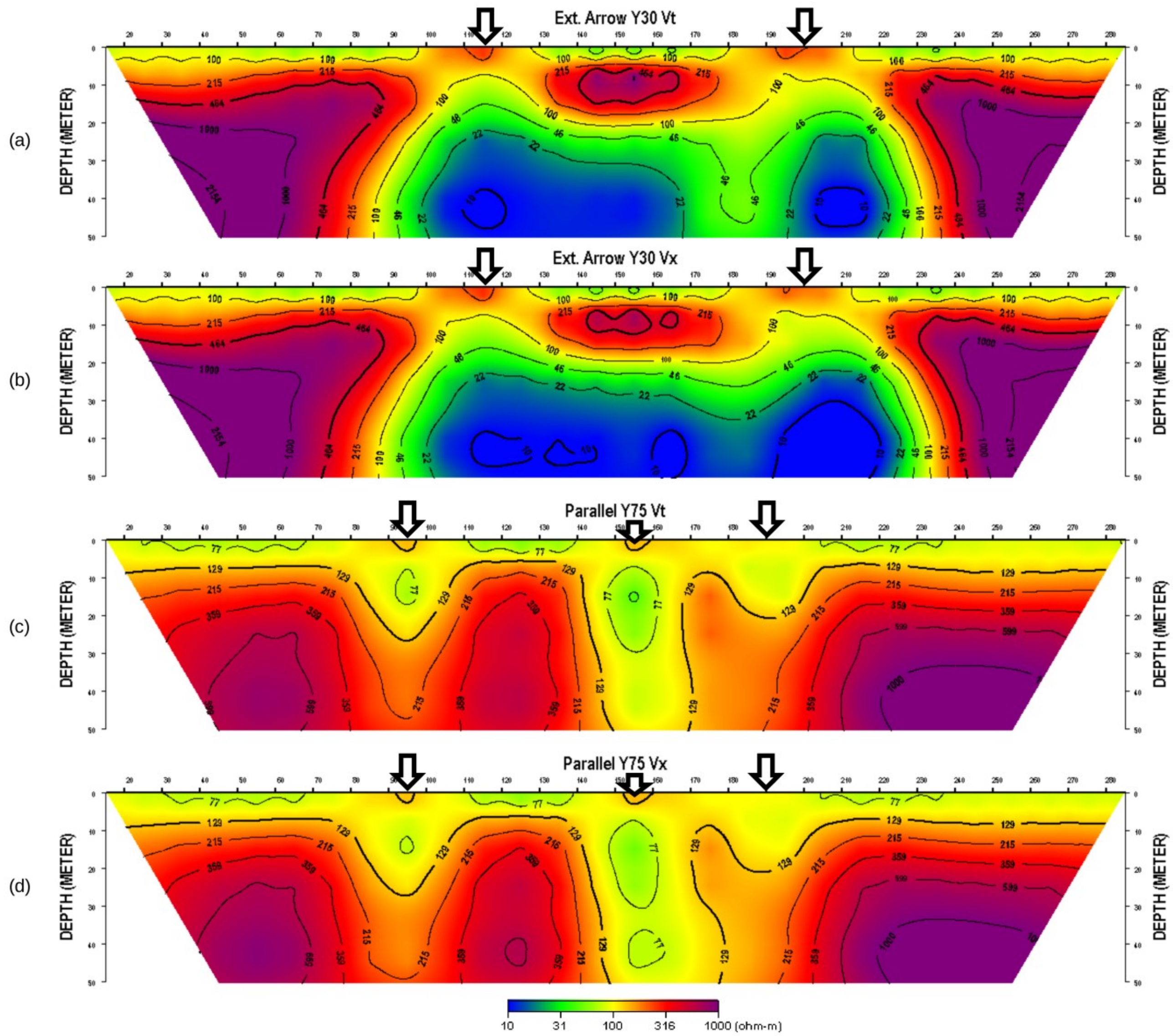


Fig. 6. Representative 2D inversion results for the quasi-2D models shown in Fig. 5: (a) and (b) Y30 survey line for the extended arrow-shaped model, and (c) and (d) Y75 survey line for the parallel anomaly model. Panels (a) and (c) show Vt-based inversion results, whereas panels (b) and (d) show Vx-based results. Both models have a resistivity contrast of 1000:1.

## CONCLUSIONS

This study examined the application of the total horizontal potential-difference magnitude (Vt), obtainable from two-component ERT data for a dipole-dipole array, to conventional 2D inversion software. This is not a complete approach that uses both the magnitude and direction of the horizontal electric-field vector within a 3D survey and inversion framework, but rather an intermediate approach intended to complement 2D interpretation based only on the conventional inline potential-difference component (Vx).

Inversion of numerically modeled data showed that, for conductive anomaly models with complex 3D geometries and strong resistivity contrasts, pronounced differences between Vt and Vx inversions can occur depending on survey-line location. In particular, in some zones such as anomaly terminations where localized 3D geometric change and electric-field directional change are both strong, Vt inversion tended to show clearer separation of adjacent low-resistivity anomalies than Vx inversion. In contrast, Vx inversion tended to produce low-resistivity zones spread broadly along the survey-line direction, making two anomalies appear as a single continuous structure.

Tests with different resistivity contrasts showed that these differences tended to become more pronounced as contrast increased. Under the low-contrast condition of 100:1, differences between Vt and Vx inversion results were small. At the base contrast of 1000:1, the difference became clear, and at the high contrast of 10000:1, anomaly separation in the Vt inversion became still more distinct. This indicates that the effectiveness of Vt-based 2D inversion is related not simply to anomaly geometry itself, but to how strongly horizontal electric-field direction changes arise under conditions of strong resistivity contrast.

For the quasi-2D structures examined, no pronounced difference was observed between Vt and Vx inversion results. When anomalies develop relatively continuously or have simple 2D continuity with respect to the survey line, the structure can be distinguished relatively well using conventional Vx-based 2D inversion alone. Therefore, the benefit of Vt inversion does not arise automatically for all 3D structures, but becomes more evident when localized 3D structures that strongly change the horizontal electric-field direction occur together with strong resistivity contrast.

Some Vt inversion sections also showed more pronounced inversion artifacts than the corresponding Vx sections. Interpretation of Vt-based 2D inversion results therefore requires distinguishing useful low-resistivity responses related to anomaly separation from artifacts that occur near section boundaries or in zones of relatively sparse data coverage. This limitation may be mitigated to some extent by interpreting the Vt results together with the corresponding Vx-based inversion results.

Overall, under the dipole–dipole array conditions examined in this study, Vt-based 2D inversion should not be regarded as a general replacement for conventional Vx-based 2D ERT. Rather, it can be considered a practical complementary approach under conditions where strong resistivity contrasts and localized 3D geometric changes are expected. Because two-component measurements provide both Vx and Vt data, the two inversion results can naturally be compared in parallel. Such comparison may provide additional grounds for interpretation of complex conductive anomalies. However, this complementary effect may depend on the geometry of the electrode array. In arrays where the potential-electrode pair is located between the current electrodes, the dominant electric field may be formed largely along the current-electrode direction, reducing the contribution of the transverse component. In such cases, the difference between Vx and Vt data may also become relatively small. Therefore, the present results should be understood as characteristics obtained under dipole–dipole array conditions, and the applicability of Vt-based 2D inversion to other electrode arrays should be evaluated through further investigation.

In this study, only the magnitude information contained in two-component measurements was used within a 2D inversion framework. Therefore, if a full 3D inversion framework that directly uses both the magnitude and direction of the horizontal electric-field vector is developed, some of the limitations observed here may be reduced, allowing complex 3D structures to be represented more accurately.

## REFERENCES

Jo, C. H., and Cho, I.-K., 2025, 3D electrical resistivity tomography via horizontal electric field component, Geophysics and Geophysical Exploration, 28(3), 97-104. (in Korean with English abstract)

Yi, M.-J., Kim, J.-H., and Chung, S.-H., 2003, Enhancing the resolving power of least-squares inversion with active constraint balancing, Geophysics, 68, 931-941.